Austin Journal of Nanomedicine & Nanotechnology

Austin Publishing Group

Open Access Full Text Article

Research Article

Higher Performance Metal-Insulator-Metal Diodes using Multiple Insulator Layers

Aydinoglu F[1,3], Alhazmi M[1,3], Cui B[2,3], Ramahi OM[3], Irannejad M[1,3], Brzezinski A[1,3] and Yavuz M[1,3*]

[1]Department of Mechanical and Mechatronics Engineering, University of Waterloo, Canada

[2]Department of Electrical and Computer Engineering, University of Waterloo, Canada

[3]Waterloo Institute for Nanotechnology, University of Waterloo, Canada

***Corresponding author:** Yavuz M, Department of Mechanical and Mechatronics Engineering, University of Waterloo, Canada and Waterloo Institute for Nanotechnology, University of Waterloo, Canada, E-mail: faydinog@uwaterloo.ca

Received: December 05, 2013; Accepted: December 27, 2013; Published: December 31, 2013

Abstract

It is found that by repeating two insulator layers with different electron affinities and keeping the total insulator thickness constant, the asymmetry and nonlinearity values can have significant impact on the behavior of Metal-Insulator-Metal diodes. The asymmetry value of a diode with a double insulator layer was recorded as 3, however, for a quadra insulator layer diode; the asymmetry value was recorded as high as 90. The new MIM diode design promises a strong impact on emerging applications such as energy harvesting from fast switching electromagnetic waves.

Keywords: Metal-Insulator-Metal diodes; Schottky diodes

Introduction

A rectifier with a high response time is critical for energy harvesting, infrared detectors, hot electron transistors [1,2], liquid-crystal display backplanes [3], macro-electronics [4], field-emission cathodes [5], and switching memories [6]. Schottky diodes are commonly used in these applications because of their fast response time. However, Schottky diodes do not operate efficiently at high THz frequencies. A Metal-Insulator-Metal (MIM) diode, which is a thin insulator layer sandwiched between two metals, is superior to Schottky diodes beyond the 12 THz [7]. The cut-off frequency of the diode is inversely proportional to the junction area of the diode. A MIM diode can operate at high Hz frequencies by reducing the junction area to nano-scale. Bareiss et al. [8] fabricated 93 nm diameter MIM diodes and claimed that these nano-scale diodes can properly operate up to 219 THz. MIM diodes can operate at the THz range due to their femto-second fast transport mechanism of quantum tunneling [9]. The tunneling phenomenon is one of the most important factors in MIM diodes. The thickness of the insulator changes the tunneling efficiency exponentially [10]. To achieve tunneling, the thickness of the insulator should be less than 10 nm [11]; however, to make the tunneling efficient, the thickness should be further reduced. The insulator layer of the diode can be grown in different ways including sputter oxidation, vapor deposition, thermal oxidation, anodic oxidation, electron-beam deposition and atomic layer deposition. Atomic layer deposition (ALD) is considered as the best way to provide uniform, pinhole free and ultra-thin oxide layers. This highly controllable deposition process makes this technique highly compatible for the growth of the insulator layer of the MIM diodes.

In addition to the operation frequency and the tunneling efficiency, the current-voltage (I-V) curve is another important parameter in determining the diode's performance. An ideal diode has to have an asymmetrical I-V curve to achieve rectification. The asymmetry is simply defined as forward current divided by reverse current ($|I_F / I_R|$). A MIM diode could have an asymmetric I-V curve if a single insulator is sandwiched between two different metals since each side has a different barrier height value, φ, which is a potential difference between the two materials. Another significant characteristic in I-V curve is turn-on voltage.

The diode's non-linearity is given by:

$$\left(\frac{dI}{dV}\right)\frac{V}{I} \tag{1}$$

Where dI, dV, I and V are variations in current, variation in voltage, current and voltage respectively. High non-linearity and high asymmetry cannot be achieved by a single insulator layer in MIM diodes [10]. MIM diodes with double insulator layers can overcome this challenge [10]. The barrier height value at each interface plays the key role regarding the tunneling efficiency, asymmetry and non-linearity in MIM diodes. The barrier height value is defined as the difference between the work function Φ of the metal and the electron affinity χ of the insulator at metal-insulator interfaces and is the difference between two electron affinity values of the insulators at insulator-insulator interfaces. If there is only one insulator used, there will be two different potential barrier values which are between metal one and the insulator, and between the metal two and the insulator. These two interfaces determine the turn on and breakdown voltages depending on the work functions of the metals. If there are two insulators, there will be three different barrier height values. If the order of the insulators is changed, the I-V characteristics will also be changed due to the change in barrier height at each interface.

In this work, a series of MIM diodes with double and four insulator layers, metal-insulator-insulator-metal (MI^2M), and metal-insulator-insulator-insulator-insulator-metal (MI^4M) were fabricated and characterized, in order to observe the impact of the number of insulators in a MIM diode performance.

Experiment

The MI^2M's bottom metal, M_1, was chosen as Chromium (Cr),

Yavuz et al. © All rights reserved

Citation: Yavuz M, Alhazmi M, Cui B, Ramahi OM, Irannejad M, et al. Higher Performance Metal-Insulator-Metal Diodes using Multiple Insulator Layers. Austin J Nanomed Nanotechnol. 2013;1(1): 1004.

and the top metal, M_2, were considered Titanium (Ti), based on their work functions properties. The insulator layers TiO_2 and Al_2O_3 were considered due to their difference in the electron affinity. Conventional photolithography followed by electron beam evaporation and atomic layer deposition (ALD) techniques, were used to fabricate the MIM diodes on the SiO_2 substrate.

A 60 nm thick Cr was deposited on a SiO_2 substrate by e-beam evaporation. After a lift-off process, insulator layers were deposited by ALD. The 34 cycles of the TiO_2 and 14 cycles of the Al_2O_3 were deposited by one atom layer by one atom layer (see supplementary information), at deposition rate of 0.044 nm/cycle and 0.105nm/cycle, respectively for TiO_2 and Al_2O_3. The total thickness of the insulator layers in the MI^2M diode was 3 nm, with each single insulator layer thickness of 1.5 nm. After a second photolithography process, 100 nm Ti was deposited by e-beam evaporation technique. A second lift-off process was performed to remove the photoresist and un-patterned areas of the second metal. The oxide layers onto the M1 were removed by using the reactive ion etching (RIE) process with Ar. The MI^4M diode with, the same bottom and top electrodes as MI^2M structure were fabricated with the procedure as aforementioned except that 17 cycles of the TiO_2, 7 cycles of the Al_2O_3, 17 cycles of the TiO_2, 7 cycles of the Al_2O_3, respectively, were deposited by ALD as insulator layers. Therefore, in the MI^4M diode, the thickness of each insulator layer was 0.75 nm, and the total thickness of the insulator layer in the MI^4M diode was 3 nm which was the same value used in the MI^2M diode. A schematic diagram of the fabricated Cr/TiO_2/Al_2O_3/Ti MI^2M diode and Cr /TiO_2/Al_2O_3/TiO_2/Al_2O_3/Ti MI^4M diode are shown in Figure 1.

Results and Discussion

The MI^2M diode and MI^4M diodes were fabricated by keeping the total thickness of the insulator layer as 3 nm to investigate the impact of the number of insulator layers on the electrical properties of the diodes. There are three different interfaces between two metals in the MI^2M diode. Each interface has a different potential barrier value. Figure 1b shows the energy band diagram of the MI^2M diode without applying any voltage. The shape of the energy band diagram was determined by the work functions and the electron affinities. The electron affinity of the insulators changes with the thickness [12] and film morphology. The electron affinities of the ALD deposited TiO_2 and Al_2O_3 of 15 nm thickness are 3.9 eV (χ_1) and 2.8 eV (χ_2), respectively. The work function of the Cr was 4.5 eV (φ_1), and that of Ti was 4.33 eV (φ_2). Therefore, the barrier heights was obtained as $\Phi_1 = \varphi_1 - \chi_1 = 0.6$ eV, $\Phi_2 = \chi_1 - \chi_2 = 1.1$ eV, and $\Phi_3 = \varphi_2 - \chi_2 = 1.53$ eV. The shape of the energy band diagram also changes by applying a bias to one of the metals. When a negative bias was applied to the Ti, the probability of an electron tunneling from Ti to Cr becomes higher than from Cr to Ti (Figure 1c). However, the tunneling probability of an electron tunneling from Cr to Ti becomes greater than from Ti to Cr when a positive bias is applied to the Ti as shown in Figure 1d.

Figure 1e, depicts a schematic diagram of the MI^4M diode. As can be seen from this figure, there were five potential barrier interfaces between the Cr and Ti. Under the zero bias, the energy band diagram of the MI^4M diode was a mixture of the metals and insulator layers bandgap as it is shown in Figure 1f. The electron affinity of ALD barrier height TiO_2 Al_2O_3 were 4.3 eV (χ_3) and 3.5 eV (χ_4), respectively. The barrier heights were obtained as $\Phi_4 = \varphi_1 - \chi_3 = 0.2$ eV, $\Phi_5 = \Phi_6 = \Phi_7 = \chi_3 - \chi_4 = 0.8$ eV, and $\Phi_8 = \varphi_2 - \chi_4 = 0.83$ eV.

However, under the bias voltage of -1V, the amplitude of the current was higher in the MI^4M diode than the MI^4M diode due to the difference in the tunneling distances. In the case of MI^2M, there was an Al_2O_3 barrier of thickness of 1.5 nm, which resulted to an energy level higher than +1 V as it was shown in Figure 1c. While in the case of using four insulator layers, there were two layers of the Al_2O_3 of thickness of 0.75 nm, which resulted to an energy level larger than -1 V, as it was, depicts in Figure 1g.

On using the applied bias voltage of +1V to the Ti, the energy levels of the Al_2O_3 and TiO_2 were higher than +1 V at the MI^2M diode as it is clear from Figure 1d. In the case of MI^4M diode structure, there were fewer barriers above +1 V, so the tunneling probability at the MI^4M diode was higher than the MI^2M diode as it was shown in Figure. 1h. Hence, at +1 V, the positive current density at the MI^4M diode was greater than the MI^2M diode. From comparison of Figure

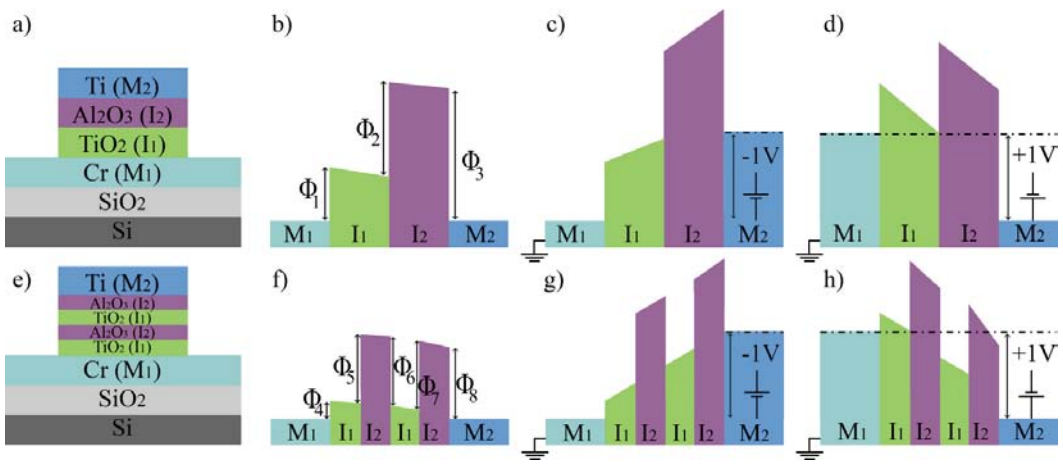

Figure 1: (a) A schematic diagrams of the cross-sectional view of the MI^2M diode. Energy band diagram of the MI^2M diode: (b) no bias applied; (c) negative; (d) positive bias applied to Ti; (e) A schematic diagrams of the cross-sectional view of the MI^4M diode. Energy band diagrams of the MI4M diode; (f) no bias applied; (g) negative; (h) positive bias applied to Ti.

1c and Figure1d under the same bias conditions, it can be concluded that the difference in the energy band diagram leading to asymmetry in MIM diodes. The same effect was also observed for the MI^4M diode as it can be seen from Figure 1g and Figure 1h.

The fabricated diodes have been characterized by a Keithley 4200-SCS Semiconductor Characterization System. The results for the I-V curve, asymmetry and non-linearity of the $Cr/TiO_2/Al_2O_3/Ti$, MI^2M, and $Cr/TiO_2/Al_2O_3/TiO_2/Al_2O_3/Ti$, MI^4M, diodes were shown in Figure 2. It was found that more current value was recorded the MI^2M diode than the MI^4M diode below -1 V (Figure 2a), which was in agreement with the energy band diagram models that was shown in Figure 1c and Figure 1g. This could be attributed to the similar break-down voltage in MI^2M diode than that in the MI^4M diode.

The MI^4M diode was shown more current than the MI^2M diode above +1 V bias. At +1.8 V, the current was recorded as 0.17 μA, and 0.85 μA respectively in the MI^2M and Mi^4M diodes. It was also found

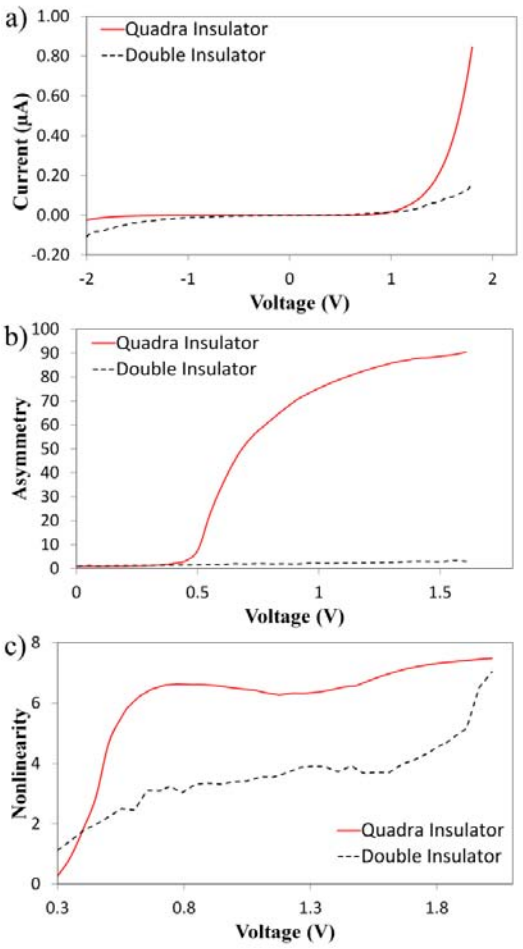

Figure 2: (a) Current – Voltage (I-V) curve (b) asymmetry (c) nonlinearity of the MI^2M and MI^4M diodes.

that the MI^4M diode was performed higher turn-on voltage than that of MI^2M one, as it was shown in Figure 2a.

A figure of merit that was used to indicate the rectification potential of the diode was the asymmetry value which was obtained as 3 at +1.6 V for the MI^2M diode. In the case of MI^4M diode, the asymmetry value was calculated as 90 at the same applied voltage. This represents a 30 times larger compare to the MI^2M diode as it was shown in Figure 2b. The nonlinearity of the MI^4M diode, as seen in Figure 2c, was clearly higher than that of the MI^2M diode over the applied voltage range of +0.4 V to +2V. This confirms that the MI^4M diode was superior to the MI^2M diode despite both diodes having an insulator layer of thickness of 3 nm.

Conclusion

A MIM diode structure with of four insulator layers was fabricated for the first time. It was shown that a metal-4 insulator-metal diode was depicted better performance than a metal-insulator-insulator-metal diode. It was showed that in case applying negative bias voltage to Ti, the probability of an electron tunneling from Ti to Cr becomes higher than from Cr to Ti. However, the tunneling probability of an electron tunneling from Cr to Ti becomes greater than from Ti to Cr when a positive bias is applied to the Ti. More current value was measured in the MI^4M diode than the MI^2M diode above +1 V bias. At +1.8 V, the current was recorded as 0.17 μA, and 0.85 μA respectively in the MI^2M and MI^4M diodes. It was also reported that the MI^4M diode was revealed better turn-on voltage than that of MI^2M one and performs a 30 times larger asymmetry than MI^2M diode.

References

1. Hartman TE, J. Appl. Phys. 1962; 33:3427.
2. Heiblum M, Tunneling hot electron transfer amplifiers /theta/ - Amplifiers operating up to the infrared. Solid-State Electronics. 1981; 24: 343-366.
3. den Boer W, Active Matrix Liquid Crystal Displays (Elsevier, Amsterdam, 2005), p. 43-47.
4. Reuss RH, Chalamala BR, Moussessian A, Kane MG, Kumar A, Zhang DC, et al. IEEE Proceedings. 2005; 93: 1239.
5. Liu H, Chen B, Li X, Liu W, Ding Y, Lu B. A metal/insulator/metal field-emission cannon. Nanotechnology. 2011; 22: 455302.
6. Waser R, Aono M. Nanoionics-based resistive switching memories. Nat Mater. 2007; 6: 833-840.
7. Hübers HW, Schwaab GW, Röser HP, J. Appl. Phys. 1994; 75: 4243.
8. Bareiss M, Ante F, Kälblein D, Jegert G, Jirauschek C, Scarpa G, et al. High-yield transfer printing of metal-insulator-metal nanodiodes. ACS Nano. 2012; 6: 2853-2859.
9. Nagae M. Response Time of Metal-Insulator-Metal Tunnel Junctions. Jpn. J. Appl. Phys. 1972; 11: 1611.
10. Eliasson BJ, PhD thesis, University of Colorado at Boulder, Boulder, 2001.
11. JGSimmons BJ, Handbook of Thin Film Technology (Eds: L. Maissel , R. Glang), (McGraw-Hill, 1970), p. 14.
12. Tien TC, Pan FM, Wang LP, Lee CH, Tung YL, Tsai SY, et al. Interfacial energy levels and related properties of atomic-layer-deposited Al2O3 films on nanoporous TiO2 electrodes of dye-sensitized solar cells. Nanotechnology. 2009; 20: 305201.

Austin J Nanomed Nanotechnol - Volume 1 Issue 1 - 2013
ISSN : 2381-8956 | www.austinpublishinggroup.org
Yavuz et al. © All rights reserved

Citation: Yavuz M, Alhazmi M, Cui B, Ramahi OM, Irannejad M, et al. Higher Performance Metal-Insulator-Metal Diodes using Multiple Insulator Layers. Austin J Nanomed Nanotechnol. 2013;1(1): 1004.